CONCEPTUAL DESIGN OF A POSITRON-ANNIHILATION SYSTEM FOR GENERATION OF QUASI-MONOCHROMATIC GAMMA RAYS*

R. J. Abrams#, C. A. Ankenbrandt, K. B. Beard, G. Flanagan, R. P. Johnson, C. Y. Yoshikawa,
Muons, Inc, Batavia, IL 60510, USA,
A. Afanasev, GWU, Washington, DC 20052, USA

Abstract

A conceptual design is presented for a system consisting of the following: an electron accelerator and production target to produce positrons, a dipole magnet and wedge to compress the positron momenta to be nearly monochromatic, a magnetic transport system to focus and direct the positrons to a converter, and a converter in which the positrons annihilate in flight to produce quasi-monochromatic gamma rays. The system represented is designed to produce ~10 MeV gammas, but it can also be tuned for other energies.

OVERVIEW

Beams of nearly monoenergetic gamma rays tunable in the energy range around 10 MeV are useful for research and for a number of industrial applications, such as for scanning of cargo for fissionable materials by inducing photofission reactions in those materials, which then are identified by detection of the delayed fission neutrons or gammas as a telltale signature of their presence [1]. The primary application of the system described is a field deployable cargo scanning system motivated by non-proliferation and homeland security. To satisfy the demands of being field deployable the system has been designed to fit within 2 standard semi-trailers.

An ideal system would provide an intense, nearly monoenergetic gamma ray beam that can be tuned to the energies of interest. In practice, an energy spread of about 1 MeV is small enough because photofission of actinide nuclei proceeds through a giant dipole resonance that is fairly broad [2].

POSITRON BEAM PRODUCTION

The electron accelerator may be one of several types, e.g. a microtron, which is more compact and relatively inexpensive compared to a linac, although a linac may be used. The optimal accelerator energy is ~75 MeV [3], and the power required to produce sufficient gamma fluxes is ~ 18 kW.

Previous simulation studies [3] carried out with G4beamline [4] have shown that the optimal target for positron production in the energy range of ~10 MeV/c by 75 MeV electrons is tungsten, 4.4 mm long.

Positrons produced in the target have a broad initial spread of momenta. The spread can be reduced by means of a dipole plus wedge, as reported previously in Reference [5], in which the target is at the entrance to a dipole magnet, and the positrons are bent 180° and impinge on a wedge that reduces the momenta in proportion to the radii of the trajectories, as shown in Figure 1.

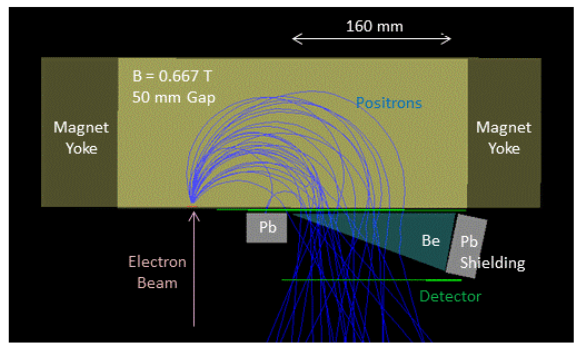

Figure 1: Sample of simulated positron tracks in dipole plus wedge. Tracks shown are those that pass through the wedge and hit simulated detectors, indicated in green.

This action produces a nearly monochromatic momentum spectrum, with a momentum spread of ~10%. The beam emerging from the wedge has RMS size 41mm by 14mm, and RMS angular spread 23° by 13° (horizontal by vertical, respectively).

POSITRON BEAM TRANSPORT

After production the positrons need to be transported to the photon production target. The beam coming out of the wedge is captured in a large aperture quadrupole triplet and then bent 90° by a dipole triplet, as shown in Figure 2, at which point it impinges on the photon production target. The positrons that do not interact in the photon production target are swept away from gamma beam.

Figure 2 shows the elements of the full system: electron beam (passing between the pole tips of the large aperture quadrupole), the target and dipole-plus-wedge subsystem, the positron beam transport, the photon production target, and the positron sweeper magnets. All of which were simulated with G4beamline.

The quadrupole triplet captures the beam and reduces its angular spread. A consequence of this is that the beam size has to grow accordingly. The inherent angular spread of the photons produced by annihilation in flight is ~ m_e/p ~50 mrad, reduction of the positron angular distributions below that value would not be beneficial. The angular spread achieved is close to the design goal of ≤ 0.1 (see Table 2). The focusing and defocusing planes are matched to the shape of the beam as it exits the wedge. In the

*This work was funded by Pacific Northwest National Laboratory which is operated for the U.S. Department of Energy by Battelle Memorial Institute under Contract DE-AC06-76RLO 1830.

boba247@muonsinc.com

configuration show in the previous figure the reducing in angle and the corresponding increase in beam size is about a factor of 4 to 6. The growth of the beam size as the positrons pass through the transport system is apparent in Figure 2.

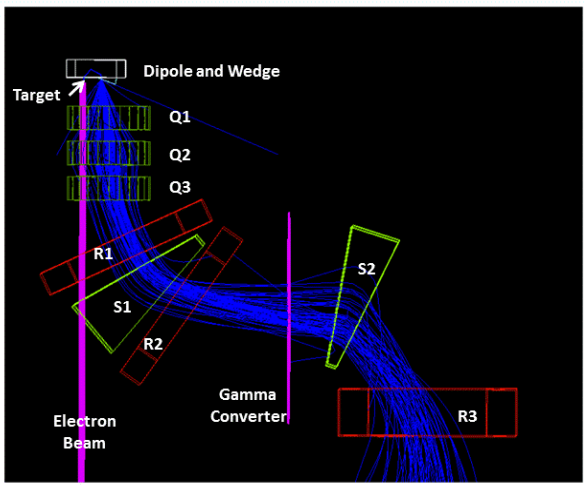

Figure 2: Positron beam transport system, viewed as transparent elements, with a beam of 15 MeV/c positrons originating from the production target in the dipole (as part of the transport tuning procedure). Photons are not displayed.

Once the beam has been made parallel it is bent 90° toward the gamma converter target. The bend is implemented with an R-S-R dipole combination. Since the weak focusing effects of the R and S magnets affect different planes the combination can be used to minimize the growth in angular spread as the beam is bent. The sweeper magnets remove the residual positrons from the path for the gammas.

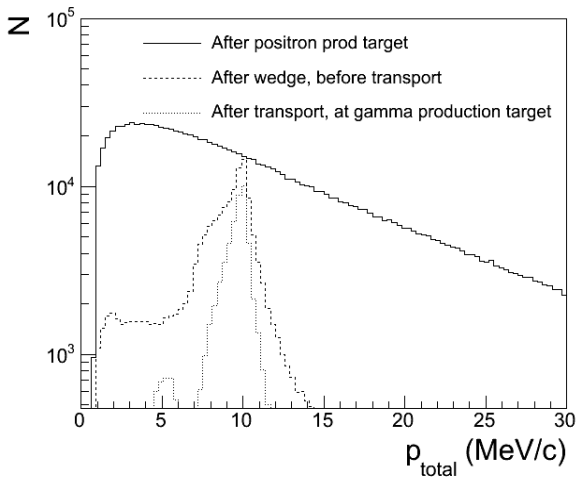

Figure 3: Momentum distributions of the positrons taken at three places in the system: just after the positron production target, after the wedge, and just before the photon conversion target.

The positron momentum spectra at three locations are shown in Figure 3. The transport system reduces the width of the positron peak and also essentially eliminates the low momentum tail present after the wedge, due to the finite momentum and angular acceptance of the transport system.

The angular spread of the positron at the same three points in the system is shown in Table 1.

Table 1: Angular Spread of Positron Beam

Location of Angular Distribution	RMS of Angular Distribution (radians)
After positron production target	0.62
After dipole-plus-wedge (before quad 1)	0.44
After positron transport (at gamma converter target)	0.14

Note that reducing the spread below ~0.1 will probably not benefit the system as the beam angles become comparable to the inherent scattering angles associated with photon production in the target.

GAMMA PRODUCTION

A study of the gamma converter and beam hardener performance was done using the end-to-end simulation framework. However, to avoid the run-time inefficiencies of producing positrons from electrons impinging on a W target we inject a positron beam between the 90° bend and the photon production target (Figure 4). The parameters of the injected beam are matched to the parameters of the beam generated from the full simulation.

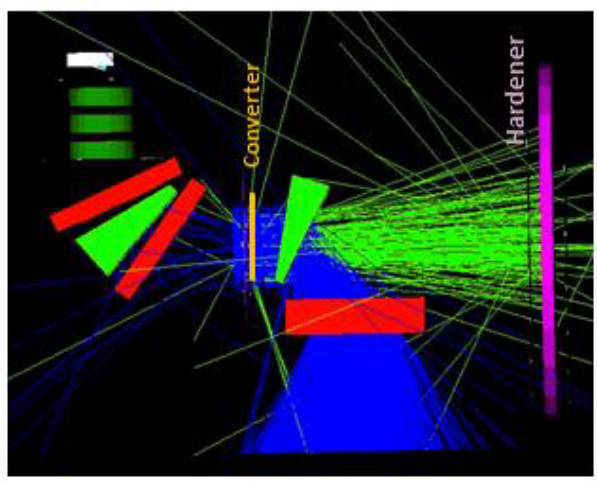

Figure 4: Layout for the simulation of positrons producing gammas in the converter and gammas passing through the beam hardener. The simulated positron beam (blue) is injected just before the converter. Gammas trajectories are shown in green.

The gammas are produced in a low-Z converter target, which enhances production by annihilation in flight and minimizes gamma production by bremsstrahlung and Compton scattering. Nearly monoenergetic positrons that annihilate in flight on the electrons in the converter yield a gamma energy spectrum that is enhanced near the

ISBN 978-3-95450-115-1

incident positron energy and aligned along the direction of the positrons [6]. This also results in a much higher proportion of gammas in the desired energy region than the spectrum resulting from bremsstrahlung from electrons impinging on a high-Z target.

The gamma energy spectra for several thicknesses of LiH converters are shown in Figure 6.

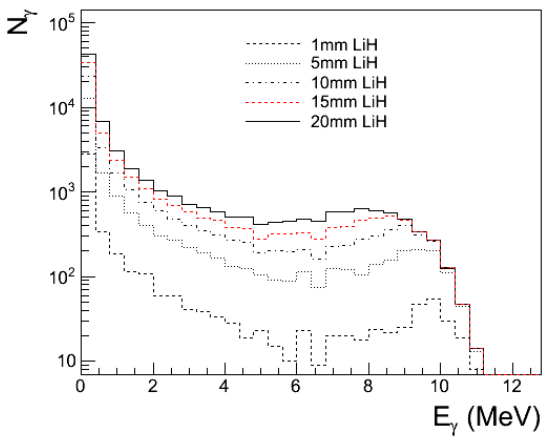

Figure 6: Gamma energy spectra for LiH converters between 1mm and 20 mm thick.

Larger converter thickness improves the conversion efficiency of positrons into photons, but degrades the energy of the positrons, contributing to larger photon energy spread. We chose the 10mm thickness as optimal. The proportion of (undesirable) low energy photons in the beam can be reduced by inserting a beam hardener after the photon conversion target. As shown in Figure 7, both Al and Be hardeners preferentially reduce the low energy peak relative to the useful energy range.

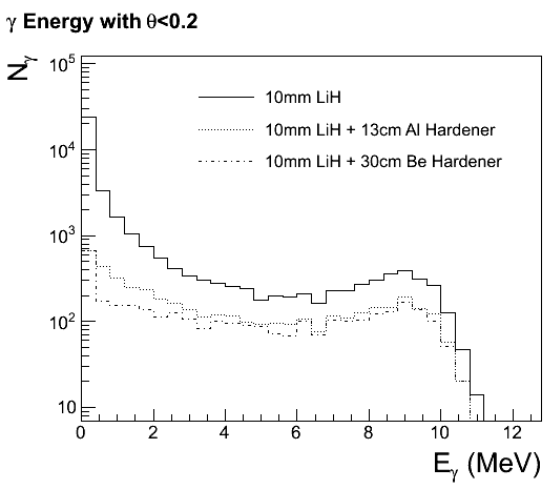

Figure 7: Gamma energy spectra for Θ < 0.2 radians, for Al and Be hardeners of equal radiation lengths.

The Al hardener reduces the number of background gammas between 0.0 and 1.2 MeV by a factor of 20 while losing only 53% of the desired gammas between 8.4 and 9.6 MeV. The Be hardener is even more effective, by reducing the background gammas by a factor of 38, while reducing the desired gammas by 58%. Considering cost and simplicity, the Al hardener is preferred.

END TO END SIMULATION RESULTS

A full end-to-end simulation was made, with a sample of 7.0×10^6, 75MeV electrons impinging on a 4.4mm thick W target, with the dipole magnet and a Be wedge pictured in Figure 1, passing through the transport system pictured in Figure 2, and a 10 mm LiH converter. The results of the simulation are summarized in Table 2. The useful gammas are those with energy greater than 6 MeV. The lower energy gammas cannot produce photo-fissions, and thus constitute an irradiation background.

To produce the desired flux of 1.5×10^{10} gammas per second for scanning ($E_\gamma > 6$ MeV) requires ~18 kW of power in the electron beam.

Table 2: Performance of the Complete System

Electrons on target	7.0×10^6
Positrons produced	1.1×10^6
Positrons out of wedge	1.6×10^5
Positrons transported to converter target	5.9×10^4
Gammas for scanning (all)	2.3×10^3 (beam spot rms (x,y) = (713mm,626mm)
Gammas for scanning (>6MeV)	4.9×10^2

REFERENCES

[1] J. L. Jones et al., Nucl. Instrum. Methods B 261 (2007) 326.
[2] J.T. Caldwell et al., Phys. Rev. C 21 (1980) 1215.
[3] C. Yoshikawa et al., these proceedings, paper MOPEA045.
[4] G4beamline, is a GEANT4-based simulation package, available at http://g4beamline.muonsinc.com
[5] R. Abrams et al., Proc. of IPAC10, paper MOPEA044 (2010).
[6] A. Afanasev et al., Proc. of IPAC10, paper MOPEA043 (2010).